

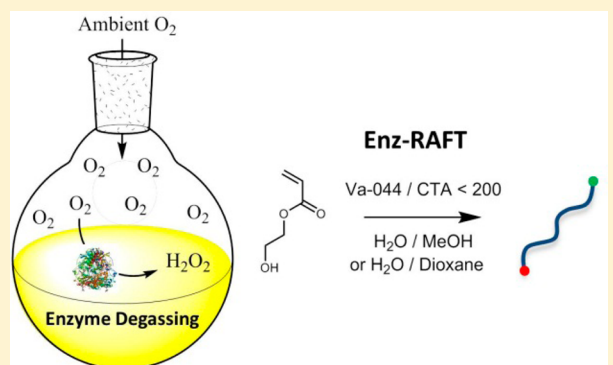
Highly Controlled Open Vessel RAFT Polymerizations by Enzyme Degassing

Robert Chapman,[†] Adam J. Gormley,[†] Karla-Luise Herpoldt, and Molly M. Stevens*

Department of Materials, Department of Bioengineering, and the Institute for Biomedical Engineering, Imperial College London, London SW7 2AZ, United Kingdom

 Supporting Information

ABSTRACT: Intolerance to oxygen is a key limitation in many reactions and particularly in controlled radical polymerizations. Here we introduce the use of enzymes such as glucose oxidase (GOx) to deoxygenate reversible addition–fragmentation chain transfer polymerizations (Enz-RAFT), facilitating the preparation of highly controlled polymers in vessels open to ambient oxygen. Because the removal of oxygen is so efficient, very low concentrations of GOx and initiator can be used, enabling excellent control which is demonstrated by pseudoliving polymerization kinetics and the preparation of multiblock copolymers with narrow molecular weight distributions ($M_w/M_n < 1.15$). GOx retains sufficient activity to facilitate polymerization not only in aqueous solutions but also in a range of water/organic solvent mixtures, and we demonstrate the use of this technique to perform open vessel Enz-RAFT polymerizations in various methanol and dioxane/water mixtures.



Controlled radical polymerization (CRP) techniques such as atom transfer radical polymerization (ATRP)¹ and RAFT^{2–4} have revolutionized the field of polymer synthesis in the past two decades by enabling the preparation of precisely defined macromolecules. One of the key limitations of all CRPs, however, is their intolerance to oxygen. Oxygen is an excellent radical scavenger and will therefore quench the propagating center in any radical polymerization and neutralize the catalyst in any ATRP-type reaction. The inherent intolerance of RAFT to oxygen not only makes polymerizations more challenging to conduct in a high throughput, or an industrial setting,⁵ but also limits the ability to gain fine control in a laboratory setting. This is because the fidelity of the polymer end groups is entirely dependent on the ratio of chain transfer agent (CTA) to initiator used. Every initiating radical introduced to the reaction will either consume oxygen or terminate, producing a dead chain devoid of the RAFT end group. In order to access highly controlled polymers, therefore, a low concentration of initiator relative to RAFT agent is required. The power of RAFT at high CTA/initiator ratios has recently been demonstrated by Gody et al., who were able to synthesize various 12–20-block copolymers with dispersities ($D = M_w/M_n$) as low as 1.4.^{6,7} This unparalleled level of control was possible in their case because the block length was small allowing the use of relatively low initiator concentrations.

In the past decade a few methods have been developed which enable CRPs to be conducted in sealed reaction vessels, in the presence of a limited amount of oxygen. In ATRP reactions, oxygen can be removed either by means of a reducing agent, as in activators regenerated by electron transfer (ARGET)

ATRP,^{8,9} or by free radicals, as in initiators for continuous activator regeneration (ICAR) ATRP.¹⁰ Photoinitiators have been widely used to enable free radical polymerizations to be conducted in aerated media,^{11–14} but because the generated free radicals are used to both quench oxygen and initiate polymerization, obtaining high control is very difficult. Boyer and co-workers have recently shown the use of photoinitiators to conduct well-controlled RAFT polymerizations in sealed vessels (which they term PET-RAFT).¹⁵ In their system radicals generated by photoirradiation of an iridium catalyst are used to consume excess oxygen prior to polymerization. However, as with the ATRP-based systems, the polymerizations will only work in sealed vessels as they rely on the use of addition radicals to scrub the oxygen before the polymerization can proceed.

Most often in nature deoxygenation is achieved by the use of enzymes. Glucose oxidase (GOx) is a highly efficient example, which consumes oxygen and generates hydrogen peroxide through the oxidation of glucose into D-glucono- δ -lactone. GOx has predominantly been exploited in polymerization reactions as a source of initiation rather than as a mechanism for oxygen consumption, by using the Fenton reaction to degrade hydrogen peroxide into hydroxyl radicals.^{16–20} In a recent study by our group, we observed that a very low concentration of GOx (200 nM) was able to entirely deoxygenate media

Received: October 16, 2014

Revised: November 14, 2014

Published: November 26, 2014

allowing for the use of polymer based amplification in nanoparticle-based biosensing applications.²¹ This observation led us to consider using this enzyme degassing system for RAFT polymerizations (which we term Enz-RAFT), where low oxygen concentrations are desirable (Figure 1). GOx is a

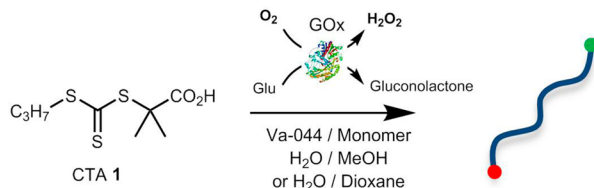


Figure 1. Schematic for open vessel RAFT polymerizations showing the chain transfer agent (CTA) 2-(propylthiocarbonothioylthio)-2-methylpropionic acid (**1**). Glucose oxidase (GOx) is used to remove the oxygen from the solution, allowing polymerization to proceed in an open vessel.

particularly attractive enzyme to use due to its high activity and compatibility with organic solvents²² and its good thermal stability.²³ GOx is also inexpensive and readily available in large quantities as it is isolated from a fungus (*Aspergillus niger*) rather than via recombinant synthesis. Unlike PET-RAFT, ARGET, and ICAR-ATRP, this mechanism for oxygen scrubbing is decoupled from the polymerization mechanism so it should be possible to polymerize both in an open vessel and at low concentrations of initiator, facilitating high control. We expect that enzyme degassing could significantly boost the synthetic power of RAFT, particularly if combined with high-throughput polymer synthesis where reliable degassing mechanisms are challenging to find.^{5,24,25}

EXPERIMENTAL SECTION

Materials. Glucose oxidase (GOx) from *Aspergillus niger* was purchased from Sigma-Aldrich as a lyophilized powder, dissolved in phosphate buffered saline (PBS), and stored in aliquots at -20°C to avoid successive freeze–thaw cycles. 2-Hydroxyethyl acrylate (HEA), methacrylic acid (MA), *N,N*-dimethylacrylamide (DMAm), and 2-hydroxypropylmethacrylamide (HPMA) were purchased from Sigma-Aldrich and deinhibited prior to use by passing it over a short column of inhibitor removal beads (for removal of MEHQ). VA-044 was purchased from Wako Chemicals and used as received. All water was deionized prior to use. All other reagents and solvents were purchased from Sigma-Aldrich and used as received. Peroxide concentration was determined using the Pierce xylanol orange aqueous quantitative peroxide assay from Thermo Scientific.

Modeling of GOx Kinetics. The concentration of oxygen within the reaction was modeled as a function of time and GOx concentration. Fick's law was used to determine the rate of oxygen diffusion and the rate of oxygen consumption by the enzyme was accounted for by Michaelis–Menten kinetics, in a similar way to our previous work.²¹ A detailed description of the equations used is given in the Supporting Information. Briefly, two scenarios were considered. In the first, molecular diffusion was assumed to be the only mass transport process, resembling an unstirred vial. In this case, the oxygen concentration over time was modeled as a function of depth from the solution surface ($z = 0$) for various GOx concentrations. The depth was split into slices of $25\ \mu\text{m}$, and at each height, oxygen diffusion in and out and consumption of

oxygen by GOx were considered. The analysis of diffusion in only one dimension allows us to neglect the effect of the surface area of the reaction vessel. Because of the complexities of calculating an oxygen diffusion coefficient which takes into account the binary nature of the solvent (methanol and water) and the addition of glucose and ionic species, we assume the diffusion coefficient to be that of O_2 diffusing into H_2O . Measurements in the literature of the effect of the presence of glucose,²⁶ and of a methanol in aqueous solutions,^{27,28} have shown the effect on the diffusion coefficient to be $<20\%$, and this level of accuracy was considered sufficient for the purposes of the model. In the second scenario, the Whitman two film model for oxygen transport was used.²⁹ This assumes the presence of an oxygenated thin film above a well-mixed bulk solution. For a small vessel mixed at high frequency (rpm >200) we can assume the bulk solution to be well-mixed, creating a homogeneous oxygen concentration and removing the depth dependence seen in the first model.^{30,31} In this instance, only diffusion of oxygen into the bulk, and consumption of oxygen by GOx were considered, and the bulk concentration of oxygen was modeled with respect only to time and GOx concentration.

Preparation of the RAFT Agent (1**).** 2-(Propylthiocarbonothioylthio)-2-methylpropionic acid (**1**) was synthesized following a similar protocol to literature.¹⁹ 1-Propanethiol (3.04 g, 40 mmol) was added into a stirred solution of potassium hydroxide (4.48 g, 80 mmol) in a water/acetone mixture (2:1 v/v, 50 mL). Carbon disulfide (CS_2 , 6.39 g, 84 mmol) was then added dropwise. After stirring for 3 h at RT, 2-bromo-2-methylpropionic acid (6.68 g, 40 mmol) was added dropwise, and the mixture was left to stir overnight. After removal of the acetone, the aqueous solution was acidified to pH 2 with HCl and extracted with CH_2Cl_3 ($2 \times 50\text{ mL}$). The combined organic fractions were washed with water ($2 \times 50\text{ mL}$) and brine ($1 \times 50\text{ mL}$) and then dried over MgSO_4 . The crude product was purified over a silica column (1:4 EtOAc:hexane, 1% acetic acid), yielding the product as a dark orange solid (3.96 g, 16.6 mmol, 42%). ^1H NMR (400 MHz, CDCl_3) δ (ppm): 3.26 (t, $J = 7.4\text{ Hz}$, 2H), 1.77–1.65 (m, 8H), 1.00 (t, $J = 7.4\text{ Hz}$, 3H). ^{13}C NMR (100 MHz, CDCl_3) δ (ppm): 220.91 (C=S), 179.18 (C=O), 55.73 (S–C_q–), 38.93 (S–CH₂–), 25.31 (CH₃–CH₂–), 21.51 (CH₃–CH₂–), 13.60 (CH₃–C_q–).

General Polymerization Protocol. A stock solution of the RAFT agent **1** in a mixture of methanol/phosphate buffered saline (PBS) (30% v/v, 200 mg/mL) was prepared and the pH was adjusted to 7. In a typical polymerization, the RAFT agent (32 mg, 0.134 mmol) was added to deinhibited HEA (0.390 g, 3.36 mmol, 25 equiv to **1**). Glucose (30 mg, 1.68 mmol, 100 mM final concentration) and VA-044 (2.2 mg, 6.71 μmol , 0.05 equiv to **1**) were added in PBS, and the solution was made up to a final monomer concentration of 2 M with methanol and PBS such that the final ratio of methanol:PBS was 1:4. In control polymerizations this solution was deoxygenated by bubbling with argon for 10 min before heating at 45°C . Samples were taken under inert conditions. For GOx degassed polymerizations, a solution of GOx in PBS (100 mM, 16 mg/mL, 16.8 μL) was added, and the solution was left at room temperature for 10 min to degas before heating at 45°C . Samples in these cases were taken by simply removing the lid and pipetting out 30 μL of solution. In the case of the dimethylacrylamide polymerizations, the pH of the solution was adjusted to 7 before addition of the GOx.

NMR Kinetics. *In situ* conversion kinetics were monitored in a 400 MHz NMR spectrometer at 45 °C by scaling the general polymerization protocol down to a total volume of 0.63 mL and replacing the PBS with PBS in D₂O. Single scan spectra were collected every 1 min.

Determination of GOx Activity. A solution of glucose in PBS (1 M, 30 μL) was diluted with PBS and either methanol, *tert*-butanol, acetonitrile, DMSO, or dioxane to a total volume of 270 μL, such that the final solvent concentrations would be 20, 40, 60 or 80% (v/v) in 1.75 mL glass vials. GOx in PBS (2 mM, 30 μL) was then added to start the reaction, and the sealed vials were placed in a heating block at 45 °C for exactly 20 min before being diluted 40-fold into PBS. In parallel, a standard curve of GOx in PBS (50, 100, 150, and 200 nM) was prepared and heated in the same way. Peroxide concentration was measured by adding 10 μL of the diluted solution to 100 μL of the xylenol orange assay buffer (1:100 of reagent A:B) and measuring the absorbance at 595 nm after 20 min.

Characterization. Conversion was determined by ¹H NMR by integration of the monomer peak at 6.3 ppm relative to the O—CH₂ group on the side chain at 4.1 ppm. In the case of dioxane polymerizations, conversion was determined by the change in monomer signal relative to a trioxane reference peak. Spectra were collected on a 400 MHz Bruker NMR spectrometer in *d*₆-DMSO. The molecular weight distributions of the polymers were characterized using size exclusion chromatography (SEC) over two PSS GRAM columns in series using DMF (+ 0.075% w/v LiBr) as the eluent. Retention times were normalized using water as a flow rate marker. Molecular weights were calculated relative to a set of narrow polystyrene standards and corrected using the Mark–Houwink (MH) parameters for polyethylene oxide ($K = 55 \times 10^{-5}$ dL/g, $\alpha = 0.643$)²⁰ in the absence of any available literature for pHEA in DMF.

RESULTS AND DISCUSSION

Optimization of Enzyme Concentration. Before using glucose oxidase (GOx) in a RAFT polymerization, we first sought to estimate the concentration of the enzyme that would be required to sufficiently degas the polymerization solution by modeling the system, building upon our previous work.²¹ Both unstirred and stirred solutions were considered (Figure 2a). In the unstirred case only transport of oxygen (O₂) via diffusion from the surface was considered, resulting in an oxygen gradient with depth. In the stirred case a homogeneous concentration of oxygen throughout the bulk solution was assumed, resulting in faster rates of diffusion. Oxygen transfer from gas to liquid phase in both stirred and nonstirred vessels has been well studied due to its relevance in fermentation and bioreactor design. The models presented here describe a simple first approximation to understanding the role of diffusion of oxygen on polymerization. For a more detailed description, excellent reviews on the mathematics involved can be found in the literature.^{27,34} The modeled O₂ concentrations at a depth of 0.5 cm from the surface vs time at varying concentrations of GOx are shown in Figure 2b,c. As can be seen, increasing concentrations of GOx resulted in a lower theoretical oxygen concentration. In both the stirred and unstirred cases the O₂ concentration is expected to reach a steady state plateau within 10 min, at which point the rate of oxygen consumption by GOx is in equilibrium with oxygen diffusion from the atmosphere. At low concentrations of GOx, stirring was seen to make little difference on the modeled concentration of oxygen, but at

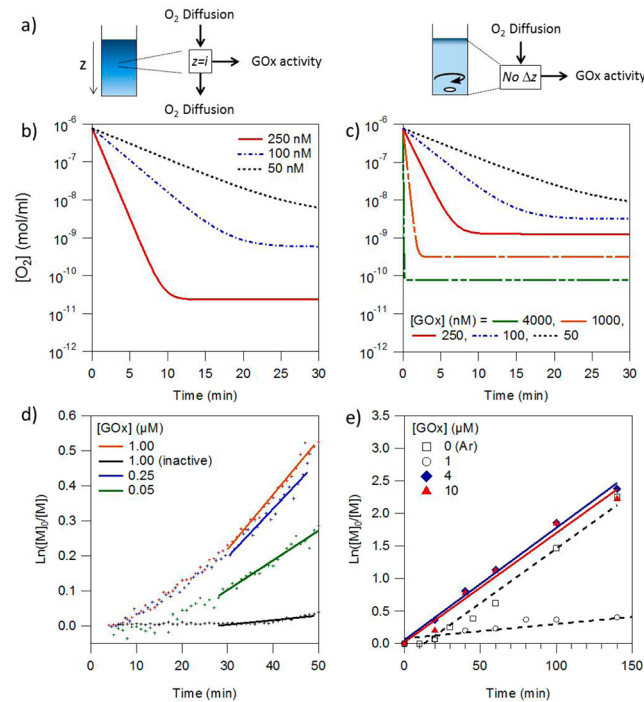


Figure 2. Modeled and measured effect of GOx on oxygen concentration. (a) Model schematic showing the parameters considered with and without stirring of the solution. (b) Modeled oxygen concentration vs time at a depth of 0.5 cm from the surface of the solution at 50–250 nM GOx. (c) Modeled bulk oxygen concentration vs time assuming homogeneous mixing at 50–4000 nM GOx. (d, e) Pseudo-first-order kinetic plots for HEA polymerizations conducted in an NMR tube without stirring [M]:[CTA] = 25 (d) or in 1.75 mL glass vials with stirring [M]:[CTA] = 100 (e). Ar = argon degassed control. [M] = 2 M in 20% (v/v) methanol/PBS, [CTA]:[VA-044] = 20, T = 45 °C.

higher concentrations of GOx, stirring was found to increase the oxygen concentration at which the plateau occurred, due to the higher rate of oxygen transport through the vessel. Previous studies on the deoxygenation of a liquid with GOx have used concentrations far in excess of that used here and measured an almost instantaneous drop in oxygen level in the bulk. At lower concentrations of GOx the same study reported that the dissolved oxygen concentration remained finite and nonzero over a 2 h experiment, in agreement with our model.²⁶

As RAFT polymerizations typically use between 0.5 and 5 mM of initiator,³⁵ we estimated that in order for polymerization to occur the oxygen concentration would need to be of the order of 10⁻⁸–10⁻⁹ mol/mL (see Supporting Information). In most cases the oxygen is removed by bubbling with nitrogen or argon, which is known to result in a concentration of dissolved oxygen of ~1 to 2 × 10⁻⁸ mol/mL.³⁶ Freeze–pump–thaw cycles are widely regarded to be the more effective method and can be used to reduce the concentration of dissolved oxygen below 1 × 10⁻⁸ mol/mL.³⁷ Our model predicts that when the solution is not stirred, 100–250 nM of GOx should be sufficient to reduce the dissolved oxygen concentration below 1 × 10⁻⁸ mol/mL, providing a level of degassing at least as good as bubbling with nitrogen and perhaps comparable to freeze–pump–thaw techniques (Figure 2b). In a stirred solution 1–4 μM GOx should be able to produce a similar effect (Figure 2c).

Kinetics of Polymerizations Degassed with GOx. To test the ability of GOx to degas the solution, we performed

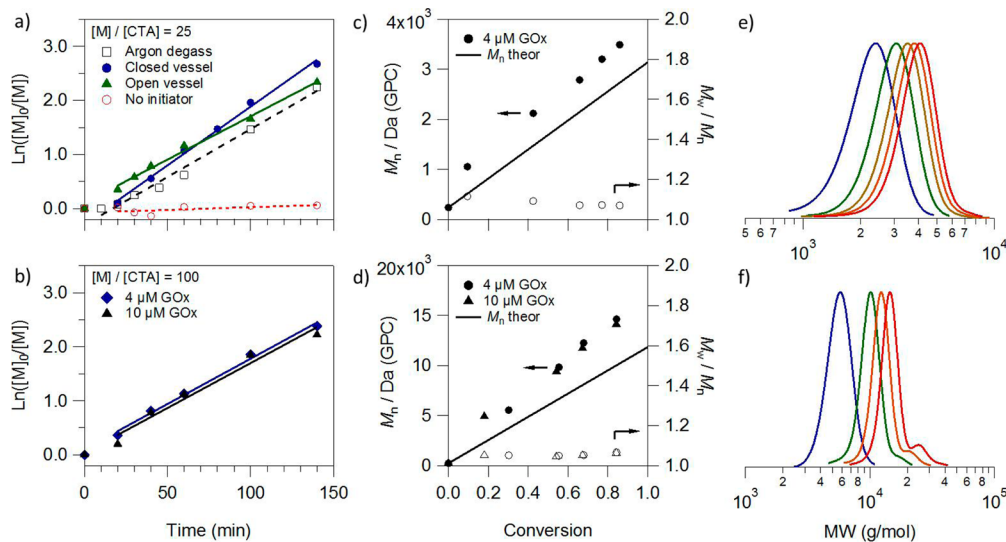


Figure 3. Kinetics of 2 M HEA polymerizations in 20% methanol/PBS degassed by GOx and stirred at 45 °C. In all cases [VA-044]/[CTA] = 0.05. (a, b) Pseudo-first-order kinetic plots with (closed symbols) and without (open symbols) GOx and VA-044 (a) $[M]/[CTA] = 25$ (1–3), (b) $[M]/[CTA] = 100$ (4, 5). (c, d) M_n (closed symbols) and D (open symbols) vs conversion as measured by DMF SEC for GOx degassed polymerizations in closed vessels (c) $[M]/[CTA] = 25$, [GOx] = 4 μM ; (d) $[M]/[CTA] = 100$. (e, f) Corresponding SEC normalized RI traces for the kinetics in (c) and (d) respectively showing a clean shift in molecular weight with conversion.

Table 1. Examples of HEA Polymers Isolated at the End of Kinetic Runs Performed with GOx^a

no.	$[M]/[CTA]$	[VA044] (mM)	[GOx] (μM)	time (h)	X (%)	M_n theor (Da)	M_n SEC ^b (Da)	D^b
1 ^c	25	5	0	2.3	89	2836		
2	25	0	4	2.3	6			
3 ^d	25	5	4	2.3	93	2941	3760	1.07
4	100	1	4	2.3	91	10773	15570	1.08
5	100	1	10	2.3	89	10589	15030	1.08

^aIn all polymerizations [HEA] = 2 M in 1:4 methanol:PBS; [VA044]/[CTA] = 0.05 with CTA 1. ^bDMF SEC using MH parameters for PEO against PS standards. ^cSample degassed with Ar. ^dSamples with and without a lid give very similar results.

RAFT polymerizations of various water-soluble monomers using a water-soluble chain transfer agent (CTA) 2-(propylthiocarbonothioylthio)-2-methylpropionic acid (**1**) and thermal initiator VA-044 in water. Reactions were initially performed using 2-hydroxyethyl acrylate (HEA, 2 M) as the monomer in a methanol:phosphate buffered saline (PBS) mixture (20% v/v) at pH 7.4. Glucose (100 mM) was added to all reactions as substrate for the GOx. This concentration is in significant excess to ensure that the concentration of glucose is effectively constant with time. Figure 2d shows the pseudo-first-order kinetics performed in an NMR tube at 50–1000 nM GOx. The rate constants for the fitted parts of the curve are shown in the Supporting Information (Table S1). Because of the high aspect ratio of the NMR tube and the slow rate of oxygen diffusion only 250 nM GOx was required to degas the solution sufficiently for polymerization to proceed. When the methanol concentration was increased to 60% (v/v), the GOx became inactive and no polymerization occurred, indicating the initiator alone was not able to produce polymerization. Similar results were observed when polymerizations were conducted without stirring in 1.75 mL glass vials (Supporting Information, Table S2). However, when the polymerization was conducted in the same vials with stirring, more GOx was required (Figure 2e). In this case, 1 μM GOx was no longer sufficient to allow polymerization to proceed and a GOx concentration of ~4 μM was required to produce similar kinetics to the control degassed with argon. It should be noted that this concentration of GOx is

still very low (0.64 mg/mL), and even if it is not removed from the final polymer, such an amount of GOx would be negligible in mass compared to the polymer itself. This assessment is confirmed by the lack of a GOx peak in the SEC data (Supporting Information, Figure S1). It should also be noted that at these GOx concentrations the amount of hydrogen peroxide produced is low, minimizing the chances of undesired side reactions. By using a xylenol orange assay, we determined the concentration of H_2O_2 after the first 15 min of incubation with GOx in PBS to be only 42 μM . The peroxide generated by 4 μM GOx over 3 h at 45 °C was found to be insufficient to cause any noticeable degradation of the RAFT agent, as evidenced by the UV-vis spectra in Figure S2 (Supporting Information).

With the concentration of GOx required established, the kinetics of HEA Enz-RAFT polymerizations in stirred 1.75 mL glass vials, performed with 4 μM GOx, were explored in more detail (Figure 3 and Table 1, entries 2–4). Polymerizations were found to proceed with identical kinetics to the argon degassed control in either a sealed or open vessel (with no lid). The kinetics were also identical at two different target degrees of polymerization (DP) of 25 (Figure 3a) and 100 (Figure 3b). It is important to note that neither GOx itself nor the hydrogen peroxide produced as a side product was found to be capable of initiating polymerization as can be seen from the control polymerization without VA-044, in which no conversion was seen (Figure 3a). Linear molecular weight

Table 2. Examples of HEA Polymerizations at Low Initiator Concentrations

no.	[MeOH] ^a (%)	[M]/[CTA]	[VA044] (μM)	[CTA]/[VA044]	[GOx] (μM)	X (%)	M_n theor (Da)	M_n SEC ^b (Da)	D^b	% living chains ^c
6	20	25	2500	40	1.0	100	3135	4570	1.05	97.5
7	20	25	500	200	1.0	96	3031	4210	1.05	99.5
8	20	25	100	1000	1.0	58	1921	2820	1.06	99.9
9	20	25	20	5000	1.0	27	1022	1760	1.08	100.0
10	20	25	0		1.0	9	500			
11	20	10	1000	200	0.5	92	1310	2380	1.09	99.5
12 ^d	15	10	1000	133	0.8	97	2323	4560	1.06	98.8
13 ^d	11	10	1000	99	1.1	>99	3485	6480	1.07	97.7
14 ^d	9	10	1000	78	1.4	>99	4646	8760	1.06	96.5

^aMethanol % (v/v) relative to PBS in polymerization. ^bDMF SEC using MH parameters for PEO against PS standards. ^cTheoretical calculation based on 100% initiator consumption at 50% initiator efficiency. ^dMultiblock chain extension polymerizations where entries 11–14 are samples from the same polymerization at the end of each block extension. Fresh initiator and an extra 500 nM GOx was added to each reaction. Reactions were not stirred and cumulative [GOx] is reported. All polymerizations conducted at [HEA] = 2 M for 20 h at 45 °C.

evolution with time was observed for all polymers, both with a target DP of 25 (Figure 3c) and 100 (Figure 3d). In all cases, narrow dispersions ($D < 1.15$) and clean shifts in distribution with no low molecular weight tailing were seen by SEC (Figures 2e,f). Strong UV signals at 305 nm were observed at the same retention times as the refractive index (RI) peaks of the polymer, indicating the presence of the RAFT trithiocarbonate end group (Supporting Information, Figure S3). The presence of both the α - and ω -end groups in the polymer was confirmed by MALDI-TOF spectrometry (Supporting Information, Figure S4). Together, these results confirm that using GOx to degas the solutions resulted in little to no adverse effects to both the kinetics and control of the polymerization. In the case of the DP 100 polymer, some high molecular weight shouldering in the SEC traces was observed at very high conversions (>80% in Figure 3f). This was probably due to bimolecular termination at this increased viscosity rather than any effect of the GOx, as the same was not seen with the DP 25 polymer (Figure 3e).

Reducing the Initiator Concentration. In all of the above experiments 1–5 mM of initiator were used, resulting in CTA/initiator ratios of 20. In RAFT reactions the fraction of living chains at the end of a polymerization, and thus the degree of control achieved, is entirely dependent on this ratio. We therefore proceeded to investigate the extent to which the concentration of initiator could be reduced before the number of radicals in the system was so low as to be quenched by the small amount of residual oxygen that was presumed to be present (Table 2, entries 6–10). Figure 4a shows the ^1H NMR of the crude reaction mixture of these polymerizations after 20 h at 45 °C. As can be seen from the decrease in the vinyl peaks at 6.5 ppm relative to the RAFT agent CH_3 group at 1.0 ppm, when 2.5 mM initiator was used full monomer conversion was seen after 20 h even at only 1 μM GOx. At 500 μM of initiator almost full conversion was observed, dropping to ~60% at 100 μM initiator, indicating that without stirring 1 μM GOx was able to degas sufficiently well for 100–500 μM initiator to be used. For a DP 25 polymer at a monomer concentration of 2 M, such initiator concentrations represent CTA/initiator ratios of 200–1000, which would be expected to produce polymers with >99.5% living chain ends (Table 2, entries 7 and 8). All polymers demonstrated narrow monomodal molecular weight distributions by SEC ($D < 1.1$, Figure 4b). The ability to generate very well controlled polymers using GOx degassing was demonstrated by the preparation of a tetrablock polymer of HEA (Table 2, entries 11–14). In these reactions, each block

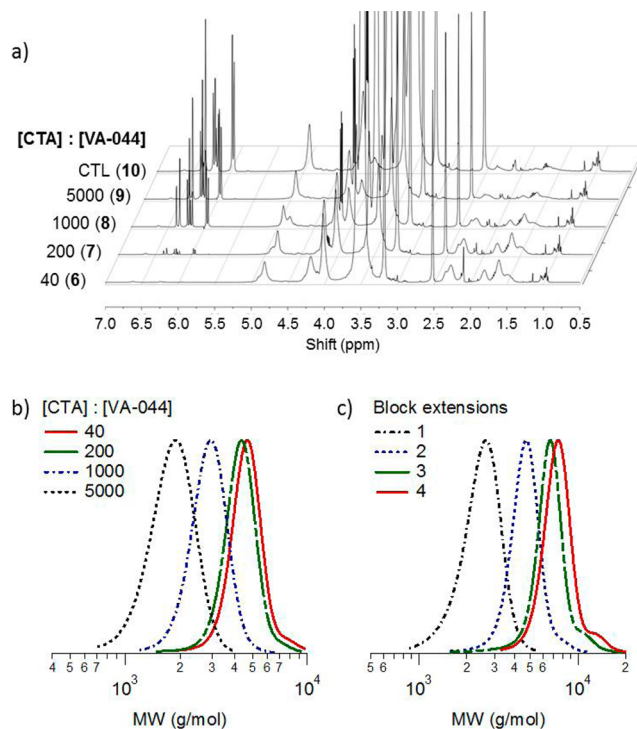


Figure 4. GOx degassed HEA polymerizations at low initiator concentrations. $[\text{M}]/[\text{CTA}] = 25$ in all cases. (a) ^1H NMR spectra ($d_6\text{-DMSO}$) of polymerization solutions containing 1 μM GOx and 0–2.5 mM VA044 after 20 h at 45 °C showing decreasing monomer signal with increasing initiator concentration (6–10) and (b) the corresponding SEC normalized RI traces, (c) SEC normalized RI traces for each block in a tetrablock polymer synthesized by three successive chain extensions with HEA (11–14). Each polymerization was performed at 45 °C for 20 h. GOx (500 nM) and VA044 (1 mM) were added for each extension. NMR are truncated for clarity.

was polymerized for 20 h to <99% conversion without stirring, at which point fresh initiator and HEA was added for the next block extension without purification. Fresh GOx (500 nM) was added for each extension, resulting in a total GOx concentration of 1.4 μM after the fourth block. The initiator concentration was maintained at 1 mM throughout, which would be expected to result in polymer with 96.5% living chain ends after the fourth block. As can be seen in the SEC traces (Figure 4c), excellent extension of the polymer at each block was achieved. No tailing of the molecular weight distribution

Table 3. Examples of Polymerizations with Various Monomers and in Organic Solvent Mixtures^a

no.	monomer	solvent ^b	[M]/[CTA]	[VA044] (mM)	time (h)	X (%)	M_n theor (Da)	M_n SEC ^c (Da)	D^c
15	HEA	M (15%)	55	2.5	4	98	6496	6770	1.06
16	DMAm	M (15%)	50	2.5	4	96	4995	3840	1.06
17	MA	M (15%)	50	2.5	20	<99	4500	d	d
18	HPMA	M (15%)	43	2.5	20	<99	6334	9990	1.22
19	HEA	D (70%)	40	4.0	2.3	90	4418	4030	1.11
20	HEA	D (50%)	40	4.0	2.3	94	4604	4470	1.08

^aPolymerizations with 2-hydroxyethyl acrylate (HEA), N,N-dimethylacrylamide (DMAm), methylacrylic acid (MA), and N-(2-hydroxypropyl)-methacrylamide (HPMA). ^bPolymerizations carried out in mixtures of PBS with M = methanol, D = dioxane (v/v % shown). ^cUsing MH parameters for PEO against PS standards. ^dDue to the acid group, the MA could not be run on the DMF column. In all polymerizations CTA 1 was used. [HEA] = 2 M, [CTA]/[VA-044] = 20, [GOx] = 4 μ M.

toward low molecular weight was observed, indicative of the high control and chain-end fidelity achieved by this system.

Expanding the Range of Monomers and Solvents.

Because the mechanism of degassing is entirely decoupled from the polymerization reaction, it should be possible to polymerize any hydrophilic monomer in this manner. The polymers listed in Table 3 (entries 15–18) demonstrate the successful polymerization of example hydrophilic methacrylate, acrylamide, and methacrylamide monomers with CTA 1, using 4 μ M GOx and relatively low initiator concentrations (2.5 mM) in a stirred vial. Methacrylic acid and N-(2-hydroxypropyl)-methacrylamide required longer polymerization times than the acrylic monomers due to their slower rates of propagation. In all cases, good conversion and control were achieved, indicating that these monomers do not inhibit GOx activity. We next characterized the compatibility of Enz-RAFT to solvent mixtures. Figure 5a shows the effective activity of 200 nM GOx in a range of organic solvent/PBS mixtures as measured by the concentration of hydrogen peroxide produced in 30 min at 45 °C. As can be seen, no loss in GOx activity was observed in *tert*-butanol or acetonitrile, even at up to 80% solvent. Conversely, GOx activity was found to drop sharply with increasing concentrations of DMSO. Methanol and dioxane mixtures both demonstrated some loss in GOx activity. At 20% methanol, the GOx activity was halved, and no activity was observed at 80%. GOx activity was maintained better in dioxane mixtures, and approximately a quarter of the original activity was retained at 80% solvent. Such a high degree of solvent compatibility opens up the possibility of using this method to polymerize more hydrophobic monomers and at higher temperatures. There have been a number of reports on the use of polymers such as poly(trehalose) and poly(acrylic acid) to stabilize the activity of enzymes,^{38,39} and we suspect that the thermal stability and solvent compatibility of GOx could be greatly improved using such approaches. Given that the Enz-RAFT polymerizations described thus far were performed in 10–20% methanol/PBS, we hypothesized that the mechanism should also work, even with unmodified GOx, in up to 80% solutions of *tert*-butanol, acetonitrile, and dioxane. As GOx was most deactivated by methanol and dioxane, we decided to compare the kinetics of our control polymerization deoxygenated by argon bubbling with identical HEA polymerizations degassed by 4 μ M GOx in 20% methanol, 50 dioxane, and 70% dioxane (v/v) in PBS (Table 1, entry 3, and Table 3, entries 19 and 20). As shown in the pseudo-first-order kinetic plot in Figure 5b, all of these reactions proceeded with identical rate, indicating equal efficiency of degassing by the GOx. As with the polymerizations in 20% methanol, the molecular weight evolution of the polymers prepared in 50% and 70% dioxane

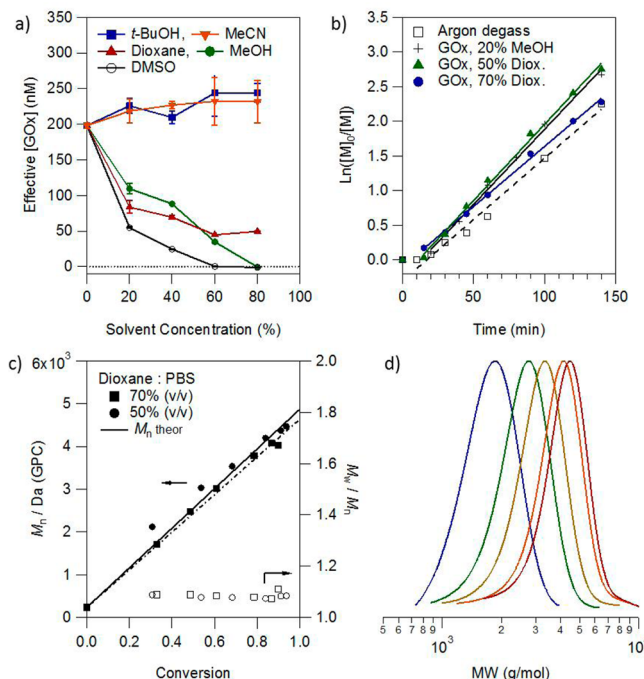


Figure 5. GOx polymerizations of HEA in organic solvent mixtures. (a) Comparison GOx activity in mixtures of PBS and methanol (MeOH), acetonitrile (MeCN), *tert*-butanol (*t*-BuOH), dioxane, and DMSO. (b) Pseudo-first-order kinetic plot of 2 M HEA polymerizations degassed with GOx in 20% methanol ([M]:[RAFT] = 25, 3) and 50–70% dioxane ([M]:[RAFT] = 40, 19–20). [GOx] = 4 μ M and [CTA]/[VA044] = 20 in each case. (c) M_n and D vs conversion as measured by DMF SEC for polymerizations in dioxane and (d) the corresponding SEC curves at increasing conversion for the 70% dioxane polymerization.

were linear with conversion (Figure 5c), and narrow molecular weight distributions were observed by SEC ($D < 1.10$, Figure 5c,d). This demonstrates the extraordinary tolerance of GOx to even high concentrations of organic solvents and opens up the possibility of polymerizing more hydrophobic monomers by this method.

CONCLUSIONS

The use of GOx for enzyme degassing of RAFT polymerizations (Enz-RAFT) has been described, facilitating highly controlled radical polymerization in an open vessel. The high activity of GOx means that only 1–4 μ M of enzyme is required to fully degas the system, in agreement with modeled enzyme kinetics. Because the enzyme degassing is completely decoupled from the polymerization mechanism, very low concentrations

of initiator can be used, resulting in excellent control and high end group fidelity in the final polymer. This enabled the preparation of a tetrablock copolymer with $D < 1.10$ without any external degassing and the polymerization of a range of hydrophilic monomers. GOx was also found to be very robust to additions of organic solvents, retaining high activity in up to 80% *tert*-butanol, acetonitrile, and dioxane. Given the low cost of GOx and ease of solution degassing with this technique, we suspect this method may also have significant large-scale industrial value.

■ ASSOCIATED CONTENT

S Supporting Information

Detailed information about the model; Figures S1–S4 and Tables S1 and S2. This material is available free of charge via the Internet at <http://pubs.acs.org>.

■ AUTHOR INFORMATION

Corresponding Author

*E-mail m.stevens@imperial.ac.uk; Ph +44 (0)20 75646804 (M.M.S.).

Author Contributions

[†]R.C. and A.J.G. contributed equally.

Notes

The authors declare no competing financial interest.

■ ACKNOWLEDGMENTS

This work was supported by a Whitaker International Scholarship to A.J.G. and EPSRC grant (EP/K020641/1). The authors are grateful to Peter Haycock for assistance with ¹H NMR kinetics as well as to Roberto de la Rica for useful discussions during the development of the work.

■ ABBREVIATIONS

CRP, controlled radical polymerization; RAFT, reversible addition–fragmentation chain transfer; ATRP, atom transfer radical polymerization; CTA, chain transfer agent; GOx, glucose oxidase; SEC, size exclusion chromatography; NMR, nuclear magnetic resonance.

■ REFERENCES

- (1) Matyjaszewski, K. *Macromolecules* **2012**, *45*, 4015–4039.
- (2) Perrier, S.; Takolpuckdee, P. *J. Polym. Sci., Part A: Polym. Chem.* **2005**, *43*, 5347–5393.
- (3) Moad, G.; Rizzardo, E.; Thang, S. H. *Aust. J. Chem.* **2006**, *59*, 669–692.
- (4) Moad, G.; Rizzardo, E.; Thang, S. H. *Aust. J. Chem.* **2009**, *62*, 1402–1472.
- (5) Guerrero-Sánchez, C.; Keddie, D. J.; Saubern, S.; Chiefari, J. *ACS Comb. Sci.* **2012**, *14*, 389–394.
- (6) Gody, G.; Maschmeyer, T.; Zetterlund, P. B.; Perrier, S. *Macromolecules* **2014**, *47*, 3451–3460.
- (7) Gody, G.; Maschmeyer, T.; Zetterlund, P. B.; Perrier, S. *Nat. Commun.* **2013**, *4*, 1–9.
- (8) Jakubowski, W.; Min, K.; Matyjaszewski, K. *Macromolecules* **2006**, *39*, 39–45.
- (9) Jakubowski, W.; Matyjaszewski, K. *Angew. Chem., Int. Ed.* **2006**, *45*, 4482–4486.
- (10) Matyjaszewski, K.; Jakubowski, W.; Min, K.; Tang, W.; Huang, J.; Braunecker, W. A.; Tsarevsky, N. V. *Proc. Natl. Acad. Sci. U. S. A.* **2006**, *103*, 15309–15314.
- (11) Zhang, J.; Frigoli, M.; Xiao, P.; Ronchi, L.; Gra, B.; Morlet-savary, F.; Fouassier, J. P.; Gigmes, D.; Laleve, J.; Ism, D. M.; Starcky, J. *Macromolecules* **2014**, *47*, 2811–2819.
- (12) Lalevée, J.; El-Roz, M.; Allonas, X.; Pierre Fouassier, J. *J. Polym. Sci., Part A: Polym. Chem.* **2008**, *46*, 2008–2014.
- (13) Lalevée, J.; El-Roz, M.; Allonas, X.; Fouassier, J. P. *J. Polym. Sci., Part A: Polym. Chem.* **2007**, *45*, 2436–2442.
- (14) Fouassier, J.; Allonas, X.; Burget, D. *Prog. Org. Coat.* **2003**, *47*, 16–36.
- (15) Xu, J.; Jung, K.; Atme, A.; Shanmugam, S.; Boyer, C. *J. Am. Chem. Soc.* **2014**, *136*, 5508–5519.
- (16) Berron, B. J.; Johnson, L. M.; Ba, X.; McCall, J. D.; Alvey, N. J.; Anseth, K. S.; Bowman, C. N. *Biotechnol. Bioeng.* **2011**, *108*, 1521–1528.
- (17) Shenoy, R.; Tibbitt, M. W.; Anseth, K. S.; Bowman, C. N. *Chem. Mater.* **2013**, *25*, 761–767.
- (18) Hume, P. S.; Bowman, C. N.; Anseth, K. S. *Biomaterials* **2011**, *32*, 6204–6212.
- (19) Shenoy, R.; Bowman, C. N. *Biomaterials* **2012**, *33*, 6909–6914.
- (20) Johnson, L. M.; Fairbanks, B. D.; Anseth, K. S.; Bowman, C. N. *Biomacromolecules* **2009**, *10*, 3114–3121.
- (21) Gormley, A. J.; Chapman, R.; Stevens, M. M. *Nano Lett.* **2014**, *14*, 6368–6373.
- (22) Vasileva, N.; Godjevargova, T. *Mater. Sci. Eng., C* **2005**, *25*, 17–21.
- (23) Malley, J. J. O.; Ulmer, R. W. *Biotechnol. Bioeng.* **1973**, *15*, 917–925.
- (24) Haven, J. J.; Guerrero-Sánchez, C.; Keddie, D. J.; Moad, G.; Thang, S. H.; Schubert, U. S. *Polym. Chem.* **2014**, *5*, 5236.
- (25) Haven, J. J.; Guerrero-Sánchez, C.; Keddie, D. J.; Moad, G. *Macromol. Rapid Commun.* **2014**, *35*, 492–497.
- (26) Tsao, G. T. *Biotechnol. Bioeng.* **1968**, *X*, 765–785.
- (27) Cussler, E. L. *Diffusion: Mass Transfer in Fluid Systems*, 3rd ed.; Cambridge University Press: New York, 2009; Vol. 31.
- (28) Noda, K.; Ohashi, M.; Ishida, K. *J. Chem. Eng. Data* **1982**, *27*, 326–328.
- (29) Whitman, W. G. *Chem. Metall. Eng.* **1923**, *29*, 146–148.
- (30) Hanhart, J.; Kramers, H.; Westerterp, K. *Chem. Eng. Sci.* **1963**, *18*, 503–509.
- (31) Lamping, S.; Zhang, H.; Allen, B.; Ayazi Shamlou, P. *Chem. Eng. Sci.* **2003**, *58*, 747–758.
- (32) Zhang, K.; Zha, Y.; Peng, B.; Chen, Y.; Tew, G. N. *J. Am. Chem. Soc.* **2013**, *135*, 15994–15997.
- (33) Azuma, C.; Dias, M. L.; Mano, E. B. *Makromol. Chem., Macromol. Symp.* **1986**, *2*, 169–178.
- (34) Garcia-Ochoa, F.; Gomez, E. *Biotechnol. Adv.* **2009**, *27*, 153–176.
- (35) Wood, M. R.; Duncalf, D. J.; Findlay, P.; Rannard, S. P.; Perrier, S. *Aust. J. Chem.* **2007**, *60*, 772.
- (36) Butler, I. B.; Schoonen, M. A.; Rickard, D. T. *Talanta* **1994**, *41*, 211–215.
- (37) Norris, B.; Meckstroth, M.; Heineman, W. *Anal. Chem.* **1976**, *1*–3.
- (38) Mancini, R. J.; Lee, J.; Maynard, H. D. *J. Am. Chem. Soc.* **2012**, *134*, 8474–8479.
- (39) Riccardi, C. M.; Cole, K. S.; Benson, K. R.; Ward, J. R.; Bassett, K. M.; Zhang, Y.; Zore, O. V.; Stromer, B.; Kasi, R. M.; Kumar, C. V. *Bioconjugate Chem.* **2014**, *25*, 1501–1510.